Journal of the Korean Society of Marine Environment & Safety
Research Paper
Vol. 22, No. 5, pp. 564-575, August 31, 2016, ISSN 1229-3431(Print) / ISSN 2287-3341(Online) http://dx.doi.org/10.7837/kosomes.2016.22.5.564

Numerical Analysis of Added Resistance and Vertical Ship Motions in Waves for KVLCC2

Mingyu Kim* · Dong-Woo Park**†

* Department of Naval Architecture, Ocean and Marine Engineering, University of Strathclyde, 100 Montrose Street, Glasgow, G4 0LZ, UK
** Department of Naval Architecture & Ocean Engineering, Tongmyong University, Busan 48520, Korea

KVLCC2에 대한 파랑 중 부가저항과 수직운동에 대한 수치해석

김민규* · 박동우**†

* 스트라스클라이드대학교 조선해양공학과, ** 동명대학교 조선해양공학과

Abstract : *The present study provides numerical simulations to predict the added resistance and ship motion of the KVLCC2 in regular waves using the unsteady Reynolds-Averaged Navier-Stokes (URANS) and 3-D potential methods. This numerical analysis is focused on added resistance and vertical ship motions (heave and pitch) under a wide range of wave conditions at three ship speeds (design, operating and zero speeds). Firstly, the characteristics of the CFD and 3-D potential flow methods are presented to predict added resistance and ship motions in regular waves taking into account various wave conditions at design speed to provide a validation study as well as at operating and zero speeds. Secondly, analyses of added resistance and ship motion with unsteady wave patterns and time history results as simulated by CFD were performed at each ship speed. Systematic validation and verifications of the numerical computations in this study were made against available Experimental Fluid Dynamics (EFD) data including grid convergence tests to demonstrate that reliable numerical results were obtained for the prediction of added resistance and ship motion in waves. Relationships between added resistance, vertical motion and changes in ship speeds were also found.*

Key Words : *Added resistance, Ship motions, URANS, CFD, KVLCC2*

요 약 : 본 연구에서는 KVLCC2의 파랑 중 부가저항과 운동을 Unsteady Reynolds-Averaged Navier-Stokes(URANS) 방법과 3차원 포텐셜법을 이용하여 추정하였다. 수치해석은 3가지 선박속도(설계, 운항, 정지 속도)에서 다양한 파랑조건에서의 선박의 부가저항 및 수직운동(상하 및 종 동요 응답)의 추정에 대해 수행되었다. 첫째, CFD와 3차원 포텐셜 방법을 이용하여 규칙파에서의 선박속도와 파랑조건에 따른 선박의 부가저항과 운동을 추정하고 실험값과의 비교를 통해 두 수치 해석법의 특징을 살펴보았다. 둘째, CFD를 이용한 선박의 속도별 비정상 파형 분포와 선박의 부가저항 및 운동의 시간이력에 대해 해석하였다. 수치 격자계에 대한 수렴도를 확인하였고 수치계산과 모형시험 결과를 비교하여 사용한 수치 기법들을 체계적으로 검증 하였다. 이를 통해 본 연구에 적용된 수치해석법들의 신뢰성과 선속변화에 따른 파랑 중 부가저항과 선박의 수직운동에 대한 관계를 확인하였다.

핵심용어 : 부가저항, 선박운동, URANS, 전산유체역학, KVLCC2

1. Introduction

Now more than ever, reduction of ship pollution and emissions, maximization of energy efficiency, enhancement of safety requirements and minimization of operational expenditure have been required. Traditionally, ship resistance and propulsion performance in calm water has been concentrated in the ship design stage even though there have been some changes for hull form design and optimization from design draught and speed to specific range of draught and speed considering operating profile (Kim and Park, 2015). But, when a ship advances through a seaway, she requires additional power in comparison with the power required in calm water due to weather, hull fouling and ship operating conditions. This degradation of the ship performance

* First Author : mingyu.kim@strath.ac.uk
† Corresponding Author : dwpark@tu.ac.kr, 051-629-1654

in a seaway is generally called “Sea Margin” and is reported to be about 15-30 % of the power required in calm water (Arribas, 2007), whilst a 15 % sea margin most commonly applied. The added resistance due to waves is one of the major components affecting this ship performance in a seaway. Therefore, the accurate prediction of the added resistance in waves is essential to evaluate the additional power and to assess environmental impact and to design ships with better fuel efficiency in actual operating conditions with other operation measures, such as voyage planning and weather routing. Also ship motions are crucial to ensure safe navigation. Regarding the international regulations, the Marine Environment Protection Committee (MEPC) of the International Maritime Organization (IMO) issued new regulations to meet the requirements in order to improve the energy efficiency level and to reduce carbon emissions. These regulations include Energy Efficiency Design Index (EEDI) as a mandatory technical measure for new ships and Energy Efficiency Operational Indicator (EEOI) which is related to ship voyage and operational efficiency as a voluntary technical measure for ships in service. Recently, the ship speed reduction coefficient (fw) is under discussion for the calculation of EEDI in the representative sea conditions of wave height, wave frequency and wind speed (IMO MEPC, 2012; ITTC, 2014).

The added resistance and the ship motion problems in waves have been widely studied by conducting experiment and numerical simulations by the potential flow and CFD methods. For potential flow methods, there are two major analytical approaches as potential flow methods for the calculation of the added resistance using the velocity potentials; the far-field method and the near-field method. The far-field method is based on the added resistance computed from the wave energy and the momentum flux generated from a ship and is evaluated across a vertical control surface of infinite radius surrounding the ship. The first study was introduced by Maruo (1960) using Kochin function which consists of radiating and diffracting wave components and investigated in detail by Joosen (1966) and Newman (1967). Later on, the far-field method based on radiated energy approach was proposed by Gerritsma and Beukelman (1972) for added resistance in head seas and has become popular in strip theory programs due to its easy implementation. Recently, Liu et al. (2011) solved the added resistance problem using quasi-second-order approach using the developed hybrid Rankine Source-Green function method considering the asymptotic and empirical methods to improve the results in short waves.

On the other hand, the near-field method estimates the added resistance by the integration of hydrodynamic pressure on the body surface, which was first introduced by Havelock (1937) where the Froude-Krylov approach was used to calculate hull pressures. The near-field method was improved by Faltinsen et al. (1980) based on the direct pressure integration approach and the 2-D linear strip theory by Salvesen et al. (1970) with the introduction of a simplified asymptotic method to overcome the deficiency of this approach in short waves. Kim et al. (2007) and Joncquez (2009) solved the added resistance based on Rankine panel method using time-domain approach with B-spline functions and investigated the effects of the Neumann-Kelvin (NK) and Double Body (DB) linearization schemes to the added resistance problem. Recently, Kim et al. (2012) investigated the added resistance using a time-domain B-spline Rankine panel method using both near-field and far field methods in addition to the NK and DB linearization schemes for the forward speed problem.

Presently as computational facilities have become more powerful and more accessible, CFD simulations are more commonly used to predict the added resistance and the ship motions and advantageous to deal directly with large ship motions and the nonlinear flow phenomena such as breaking waves and green water without explicit approximations and empirical values. Deng et al. (2010), Moctar et al. (2010) and Sadat-Hosseini et al. (2010) predicted the added resistance of KVLCC2 in head waves using CFD method in Gothenburg 2010 Workshop. Later on, Sadat-Hosseini et al. (2013) predicted the added resistance and motions for KVLCC2 using CFDSHIP-IOWA as URANS code and Lee (2015) performed experimental study on added resistance of a VLCC for ship operating conditions in waves. In addition to researches on the prediction of the added resistance and ship motions in waves, there have been studies on reduction of the added resistance by developing hull form. Park et al. (2014) and Kim et al. (2015) modified the forebody of KVLCC2 to improve the performance of the added resistance in waves. Kim et al. (2014) revised bulbous bow of a containership to optimize hull form of a containership for both operating conditions in calm water and wave conditions by CFD simulations. Also there have been researches on the increase of the required power and the ship speed loss due to waves (Kwon, 2008; Prpić-Oršić and Faltinsen, 2012; Kim et al, 2015).

In this study, the numerical simulations for the prediction of the added resistance and the ship motions for KVLCC2 in regular waves are performed by the URANS and the 3-D potential flow methods as a validation study by comparison with experimental data. For CFD, grid convergence test are carried out to find an optimal mesh system. The added resistance and vertical ship motions (heave and pitch motions) are analysed with various wave conditions at design speed as well as operating and zero speeds taking account of operational and harbour conditions of the vessel. Unsteady wave patterns and time history results of the resistance and ship vertical motions in waves simulated by CFD are analysed at each ship speed and the relationship between the added resistance and the ship vertical motions and the change for ship speeds are investigated including viscous effect.

2. Ship particulars and coordinate system

All calculations of the added resistance and the ship motions have been performed for KVLCC2, which presents the second variant of VLCC-type vessel developed by the Korean Institute of Ship & Ocean Engineering (KRISO) and is one of benchmark hull forms to study seakeeping capability by researchers. The main particulars of the KVLCC2 are given in Table 1. For CFD simulations, the model with scale ratio of 1/80 is employed in calculations without appendages.

Table 1. Main particulars of KVLCC2

Main particulars	Unit	Ship
Length between perpendiculars (L)	m	320
Breadth (B)	m	58
Depth (D)	m	30.0
Draught (T)	m	20.8
Block coefficient (C_B)	-	0.8098
Displacement (Δ)	m^3	312,622
Longitudinal centre of gravity (LCG) from aft peak	m	171.1
Vertical centre of gravity (KG)	m	18.56

In the numerical simulations, a right-handed coordinate system (x,y,z) is adopted. Fig. 1 shows the employed coordinate system where the translational displacements in the x, y and z directions are η_1(surge), η_2(sway) and η_3(heave), and the angular displacements of rotational motion about the x, y and z axes are η_4(roll), η_5(pitch) and η_6(yaw) respectively and θ angle represents the ship's heading angle to incident waves. For head seas θ angle equals 180 degrees and for beam wave from port side equals 90 degrees.

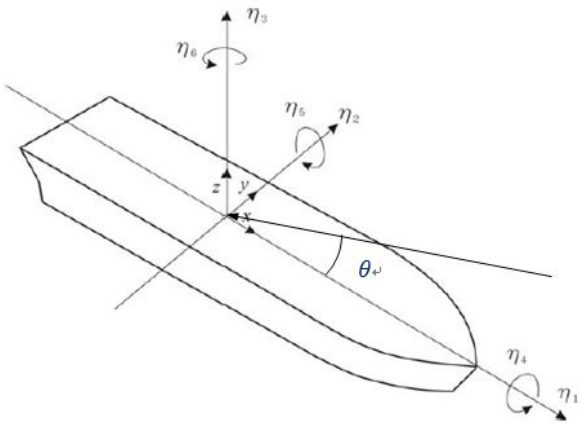

Fig. 1. Coordinate system.

3. Numerical methods and modelling

In the present study, two different methods of the 3-D linear potential flow and CFD were applied for numerical simulations on the added resistance and the ship motions in regular waves.

3.1 3-D linear potential method

3-D potential flow calculation is performed using PRECAL (PREssure CALculation) software developed by MARIN (2009), based on the planer panel approach which can calculate the seakeeping behaviour of monohulls, catamarans and trimarans. In addition to the rigid body motions, it can also calculate the deformation modes of the ships girder, internal loads, pressure on the hull and added resistance in waves. PRECAL is 3D source-sink frequency domain code capable to solve the forward speed linear Boundary Value Problem (BVP) using the Approximate Forward Speed (AFS) and the Exact Forward Speed (EFS) formulations. In this study, forward speed ship motions are solved using the AFS formulation due to its fast and accurate results. The added resistance is calculated using the near-field method based on direct pressure integration over the mean wetted hull surface using the second-order forces to calculate wave drift forces while the first-order forces and moments are calculated to

solve the ship motions. The total pressure is divided into four components which are originated from the relative water height, incident wave velocities, the pressure gradient and the rotation times inertial terms. The added resistance force due to waves is calculated in time domain by Eq. (1).

$$\Delta R_{wave} = \begin{bmatrix} -\rho \int_{H_0} \vec{\nabla}\phi^{(1)} \cdot \vec{\nabla}\phi^{(1)} \vec{n}^{(0)} ds \\ -\rho \int_{H_0} \left(\vec{\alpha}^{(1)} \cdot \vec{\nabla}\right) \left(\frac{\partial \phi^{(1)}}{\partial t} + \vec{\nabla}\phi^{(1)} \cdot \vec{\nabla}\vec{\phi}\right) \vec{n}^{(0)} ds \\ +\frac{1}{2}\rho g \int_{wl} \left(\zeta^{(1)} - \alpha_3^{(1)}\right)^2 \vec{n}^{(0)} dl + \vec{\Omega}^{(1)} \times M\ddot{\vec{X}}^{(1)} \end{bmatrix} \quad (1)$$

where the first integral stands for the water velocity contribution, second integral is the pressure gradient contribution, third integral is the relative wave height contribution and the last term is for the rotation times inertia contribution. The indices stand for the order of the forces in the force contribution formulations. H_0 represents the mean position of the ship, $\vec{\alpha}^{(1)}$ represents first order translation and rotation vector, $\vec{n}^{(0)}$ is the zeroth order normal vector calculated on the mean position vessel wetted surface and $\overline{\Omega}^{(1)}$ is the first order rotation vector. In order to derive the added resistance equation in frequency domain, oscillatory description of motion and flow is introduced and steady flow contribution is neglected. The added resistance in frequency domain is formulated by Eq. (2).

$$\Delta R_{wave} = \begin{bmatrix} -\rho \int_{H_0} \left|\vec{\nabla}\phi^{(1)}\right|^2 \vec{n}^{(0)} ds \\ -\rho \int_{H_0} \left(\vec{\alpha}^{(1)} \cdot \vec{\nabla}\right) \left(i\omega_e \vec{\nabla}\phi^{(1)}\right) \vec{n}^{(0)} ds \\ +\frac{1}{2}\rho g \int_{wl} \left|\zeta^{(1)}\right|^2 \vec{n}^{(0)} dl - {\omega_e}^2 \vec{\Omega}^{(1)} \times M\vec{X}^{(1)} \end{bmatrix} \quad (2)$$

In order to evaluate the added resistance forces all components in the integrals are approached in a perturbation series. Small parameter (ε) is introduced to define quantities in perturbation series. The perturbation series expansion of the relative wave height and the velocity potential can be formulated as Eq. (3) and Eq. (4).

$$\zeta = \zeta^{(0)} + \varepsilon\zeta^{(1)} + \varepsilon^2\zeta^{(2)} + O(\varepsilon^3) \quad (3)$$

$$\phi = \bar{\phi} + \varepsilon\phi^{(1)} + \varepsilon^2\phi^{(2)} + O(\varepsilon^3) \quad (4)$$

where 0th order quantities are time independent and are assumed to be small to satisfy the linearized free-surface condition. For the same reason time dependent parts of the series are also assumed to be small.

3.2 Computational Fluid Dynamics (CFD)

An URANS was applied to calculate the added resistance and ship motions in regular waves by the commercial CFD software STAR-CCM+. For incompressible flows, if there are no external forces (f) applied to the fluid, the averaged continuity and momentum equations are given in tensor form and Cartesian coordinates by Eq. (5) and Eq. (6).

$$\frac{\partial(\rho\bar{u}_i)}{\partial x_i} = 0 \quad (5)$$

$$\frac{\partial(\rho\bar{u}_i)}{\partial t} + \frac{\partial}{\partial x_j}\left(\rho\bar{u}_i\bar{u}_j + \rho\overline{u_i'u_j'}\right) = -\frac{\partial\bar{p}}{\partial x_i} + \frac{\partial\bar{\tau}_{ij}}{\partial x_j} \quad (6)$$

where $\bar{u}_i$ is the averaged velocity vector of fluid, $\overline{u'_i u'_j}$ is the Reynolds stresses and $\bar{p}$ is the mean pressure. For Newtonian fluid under incompressible flow, the mean shear stress tensor, $\bar{\tau}_{ij}$, is expressed as Eq. (7).

$$\bar{\tau}_{ij} = \mu\left(\frac{\partial\bar{u}_i}{\partial x_j} + \frac{\partial\bar{u}_j}{\partial x_i}\right) \quad (7)$$

where μ is dynamic viscosity.

The finite volume method (FVM) and the volume of fluid (VOF) method were applied for the spatial discretization and free surface modelling individually and no mesh motion is considered for the current study. The flow equations were solved in a segregated manner with a predictor-corrector approach. Convection and diffusion terms in the URANS equations were discretised by a second-order upwind scheme and a central difference scheme. Semi-implicit method for pressure-linked equations (SIMPLE) algorithm was used to resolve the pressure-velocity coupling and a standard $k-\epsilon$ model was applied as the turbulence model. Dynamic Fluid Body Interaction (DFBI) scheme, which is used to simulate the motion of a rigid body in response to pressure and shear forces the fluid exerts, and to additional forces defined, was applied with vessel free to move in heave and pitch directions as vertical motions.

Only half of the hull (the starboard side) with scale ratio of 1/80 and control volume was taken into account in the calculations, thus a symmetry plane forms the centreline domain face to reduce computational time and complexity. The computational domain is

$-3L < x < 1.25L$, $0 < y < 2L$, $-2L < z < 1L$ where the mid-plane of the ship is located at $y = 0$ and ship draught (T) is at $z = 0$. Each boundary conditions with generated meshes is depicted in Fig. 2. Wave damping is applied to avoid the undesirable effect of the reflected waves from side and outlet boundaries with a damping length equal to 1.25L.

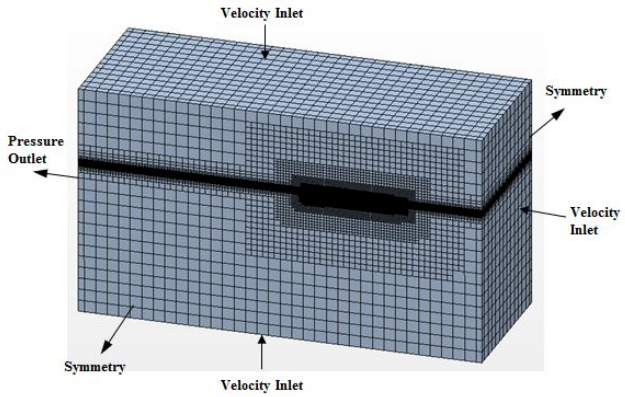

Fig. 2. Meshes and boundary conditions.

4. Discussion of results

In this section, the simulation results by CFD and the 3-D potential methods are presented by comparing with available experimental data for the added resistance and the ship motions in regular waves. Unsteady wave patterns and time history results of the resistance and ship vertical motions in waves simulated by CFD are also provided. It is noted that two vertical motions, which are Z motion (heave) and Y rotation (pitch), of all six motions are set to be free for all simulations.

4.1 Grid convergence test

Prior to the investigation on the added resistance and the ship vertical motions of heave and pitch by CFD, grid convergence test has been performed. The CFD simulations at 15.5 kts with Fn=0.142 were selected as the convergence test cases for mesh system to compare simulation results with existing experimental data for validation studies as summarized in Table 2. The wave length (λ/L) and the wave steepness (H/λ) are 1.2 and 1/60 respectively as wave conditions taking account of a resonant case (Sadat-Hosseini et al., 2013). Based on the case of the base mesh (case no. C10), the coarse and fine mesh system have been derived by a factor of $\sqrt{2}$, respectively (Bøckmann et al., 2014). The simulation time step is set to be proportional to the grid size as shown in Table 2 where Te is encountering period.

Table 2. Test cases and resistance in waves for grid convergence (λ/L=1.2, H/λ=1/60, Vs=15.5 kts)

Case no.	Mesh	λ/Δx	H/Δz	Te/Δt	Cell no.	σ_{AW}
C1C	Coarse	70	14	181	1.1E+06	5.316
C10	Base	100	20	256(2^8)	3.0E+06	5.746
C1F	Fine	140	28	362	3.9E+06	5.749

The results of the convergence test with three different mesh systems is shown in Fig 3 where ρ, g and A denote density, the gravitational acceleration and the wave amplitude respectively. As the number of cells increased, the added resistance coefficient increased especially from coarse mesh (case no. C1C) to base mesh system (case no. C10). But the results of the added resistance coefficient (σ_{AW}) for base and fine mesh (case no. C1F) were almost identical as shown in Table 2. Therefore the base mesh system (case no. C10) has been chosen for CFD simulations in this study and, according to the wave conditions, the cell number and time step differ.

The added resistance due to waves (R_{AW}) is obtained by Eq. (8).

$$R_{AW} = R_{wave} - R_c \tag{8}$$

where R_{wave} and R_c are resistance in waves and calm water.

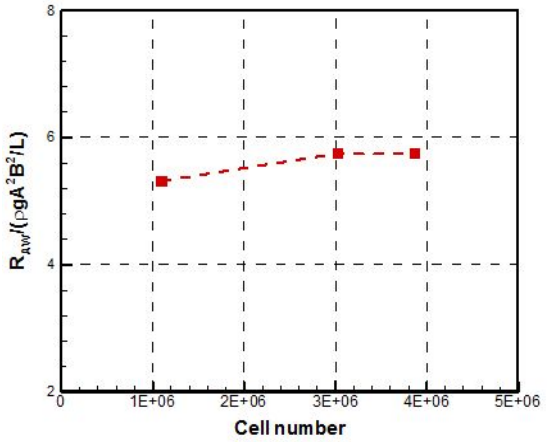

Fig. 3. Grid convergence test for the added resistance.

Fig. 4 shows the results of time history for the ship resistance, heave and pitch in waves which are oscillating well periodically corresponding to the encounter period (Te=1.3227 sec.) in Table 3.

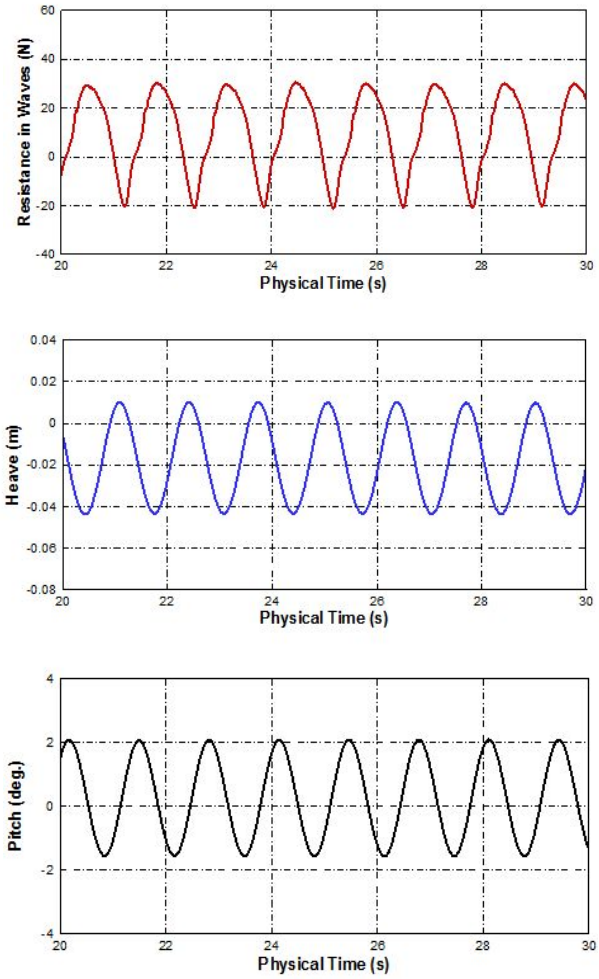

Fig. 4. Time histories of the resistance, heave and pitch in waves (case no. C10).

4.2 Added resistance and ship motions at design speed

The numerical calculations by 3-D potential method and CFD at design speed of 15.5kts with optimal mesh system after grid convergence tests are performed for various wave lengths at 1/60 of wave steepness (H/λ) including CFD simulation in calm water condition as summarised in Table 3.

The wave length (λ) is assumed by $g/(2\pi\lambda)T^2$ for deep sea and the frequency of encounter of the waves f_e for model scale is calculated by $f_e = \sqrt{g/(2\pi\lambda)} + U/\lambda$ for head sea where U denotes the ship forward speed.

Prior to the investigation on the added resistance, vertical motion transfer functions (i.e. RAO) of heave and pitch are compared with the experimental data in regular head waves from Osaka University (Larsson et al., 2010) as shown in Fig. 5

Table 3. Test cases at design speed (15.5 kts)

Case no.	Vs [kts]	Wave length (λ/L)	Wave height (H) [m]	Wave steepness (H/λ)	fe[Hz]	Te [sec.]
C00		Calm water	-	-	-	-
C10		1.20	6.40		0.7560	1.3227
C11		0.50	2.67		1.3293	0.7523
C12	15.5	0.75	4.00	1/60	1.0186	0.9818
C13		1.00	5.33		0.8476	1.1798
C14		1.40	6.40		0.6872	1.4552
C15		1.60	7.47		0.6332	1.5793

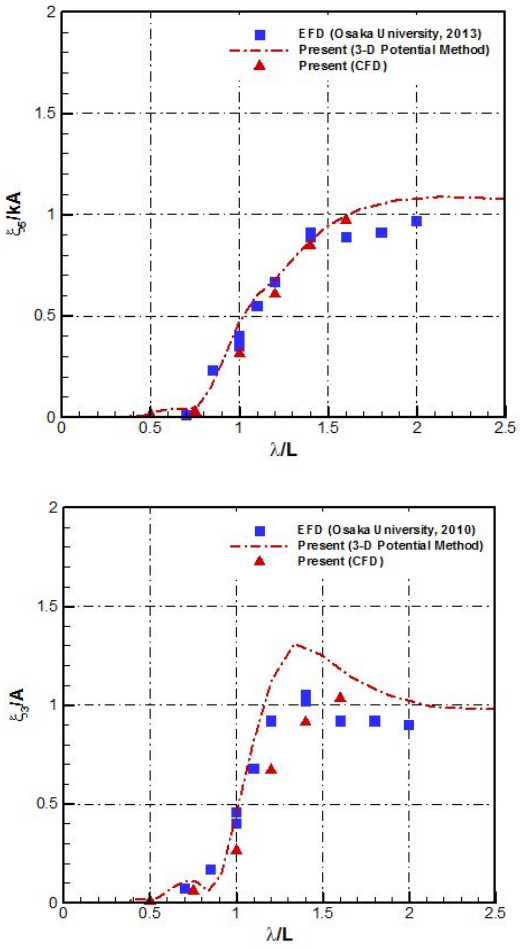

Fig. 5. Heave and pitch motion RAO (Vs=15.5kts, θ=180°).

because the added resistance due to waves is proportional to the relative motions (typically, heave and pitch motions) and inaccuracies in the predicted motions may amplify the errors in the added resistance. In this study, ξ_3 and ξ_5 are the amplitudes of heave and pitch responses respectively and $k = 2\pi/\lambda$ is the wave number in infinite depth seas. The heave and pitch motions

are evaluated at the ship's centre of gravity. The 0th and 1st order terms of the resistance force and motions calculated by CFD are used for the added resistance coefficient and motion transfer functions (Shen and Wan, 2012). 3-D potential method overestimates heave motion for peak and long waves, while CFD underestimates the heave motion slightly for the range of wave length from 1 to 1.4 even though the results of the added resistance show good agreement with experimental data as shown in Fig. 6. For the pitch motion, the calculation results of both methods show good agreement with experimental data. Overestimation of the 3-D potential method for the heave motion might be attributed to the AFS formulation, in which the BVP is solved using zero speed Green's functions and then forward speed corrections are applied to the boundary conditions, while underestimation of CFD method is likely to stem from the adoption of non-inertial reference frame in which a reference frame is undergoing acceleration with respect to an inertial frame and the laws of motion do not take the simple form they do in inertial frame. So in non-inertial reference frame, large amplitude motion causes inaccurate capturing of free surface.

The numerical results of the added resistance are compared with the experiment data (Lee et al., 2013) as illustrated in Fig. 6 which indicates that the numerical results by both numerical methods have reasonable agreement with the experimental data.

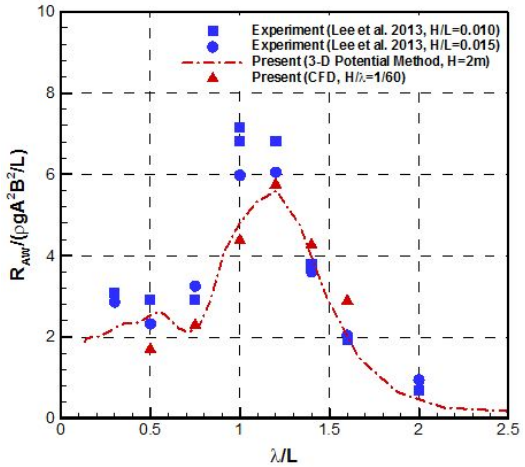

Fig. 6. Added resistance (Vs=15.5kts, θ=180°).

In order to visualise the ship motions and periodic wave patterns, four snapshots of the waves and the vessel movements were taken in a period of encounter and are displayed in Fig. 7 which shows that the phenomena of the water on deck and the bow slamming incident have been successfully captured by the current CFD model. Fig. 7(c) is the snapshot at t/Te=0.5 when the ship has the biggest added resistance as presented in Fig. 8.

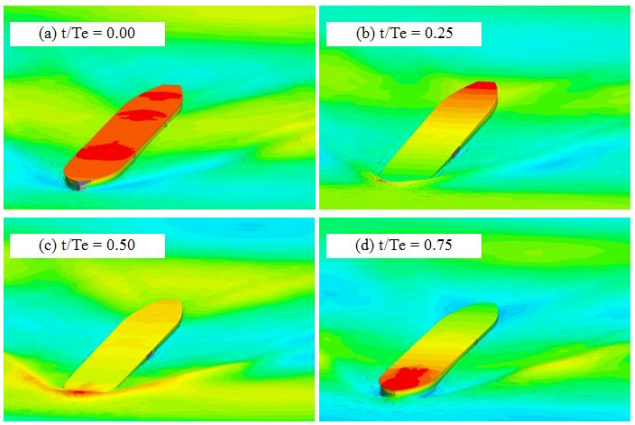

Fig. 7. Snapshots of free surface elevation over one period of encounter (case no. C10).

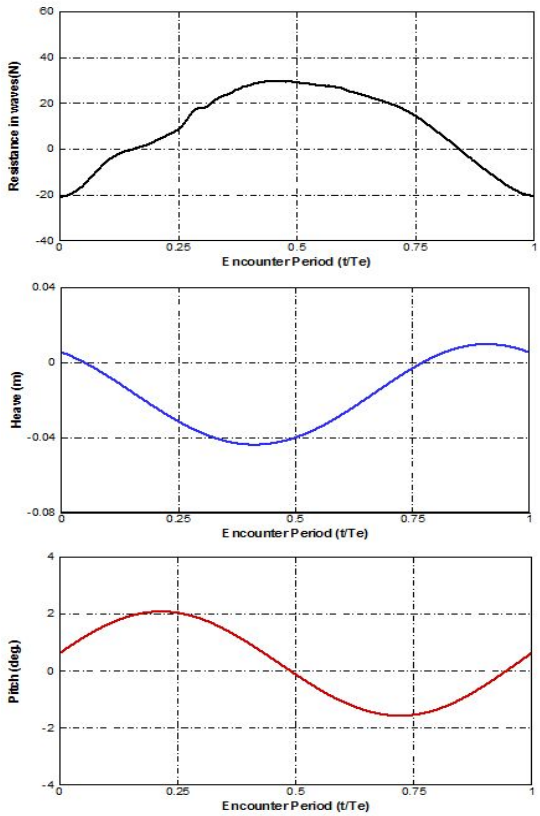

Fig. 8. Resistance, heave and pitch amplitudes over one period of encounter (case no. C10).

Similar to snapshots in Fig. 7, time histories of resistance force and heave and pitch motions are displayed over an encounter period as shown in Fig. 8. The biggest resistance force in waves is set at t/Te=0.5 when bow slamming is seen apparently at the moment wave height is high around bow with green water as depicted in Fig. 7(c) and the ship has almost lowest heave motion (i.e. sinkage) although pitch amplitude is almost zero after the bow trim. The curve of resistance force in Fig. 8 is not smooth before and after t/Te=0.25 because of the incidence of the non-linear effects of slamming and water on deck respectively.

4.3 Added resistance and ship motions at operating and zero speeds

With consideration for the slow steaming or the realistic operating speeds of the vessel, the effect of the ship speed on the added resistance and ship motions was investigated. In addition to the assumed operating speed (12kts), the cases for the zero speed (0kts) taking into account harbour condition are also simulated as summarised in Table 4. Wave conditions for wave length and height are considered the same as design speed.

Table 4. Test cases at operating (12kts) and zero speed (0kts)

Case no.	Vs [kts]	Wave length (λ/L)	Wave height (H) [m]	Wave steepness (H/λ)	fe[Hz]	Te [sec.]
C71	12	0.75	4.00	1/60	0.9515	1.0510
C72		1.00	5.33		0.7973	1.2542
C73		1.20	6.40		0.7141	1.4004
C73		1.40	7.47		0.6513	1.5355
C81	0	0.75	4.00	1/60	0.7214	1.3862
C82		1.00	5.33		0.6248	1.6006
C83		1.20	6.40		0.5703	1.7534
C84		1.40	7.47		0.5280	1.8939

Heave and pitch motions calculated by CFD are compared with the results of the 3-D potential flow method for three ship speeds as shown in Fig. 9. For heave motion, the results of the 3-D potential flow is larger than those of CFD especially for peak and long waves because they present similar characteristics of the prediction for the heave motion as shown in Fig. 5. Regarding the pitch motion, all simulation results are almost the same except λ/L=1.4 at Vs=0kts.

The added resistance in regular waves are also compared as shown in Fig 10. Numerical results by 3-D potential and CFD

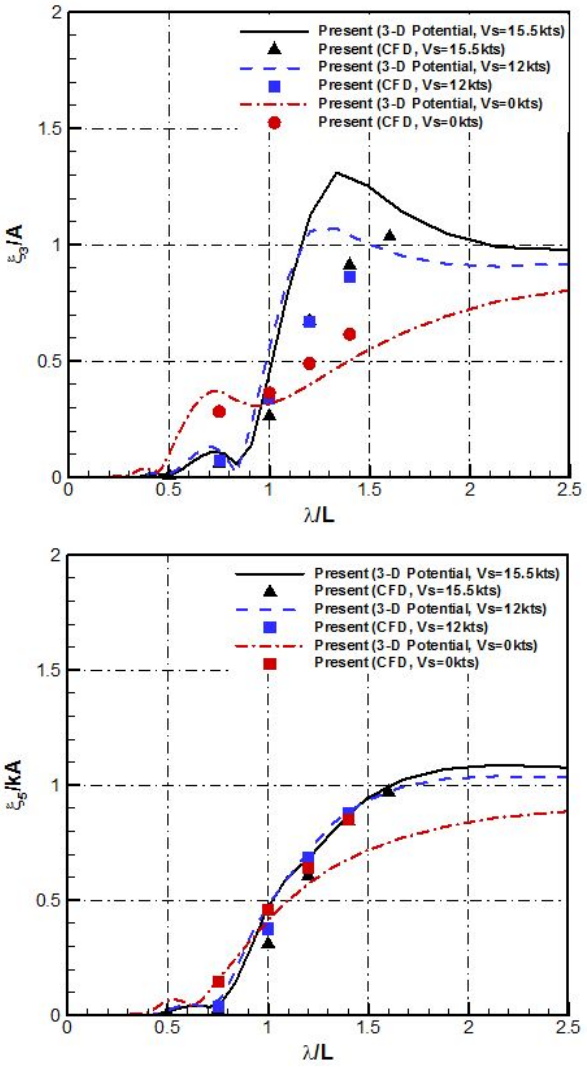

Fig. 9. Heave and pitch motion RAO with ship speeds.

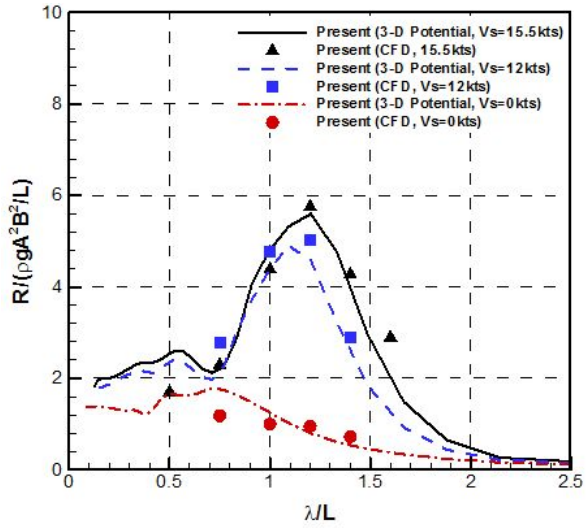

Fig. 10. Added resistance with ship speeds.

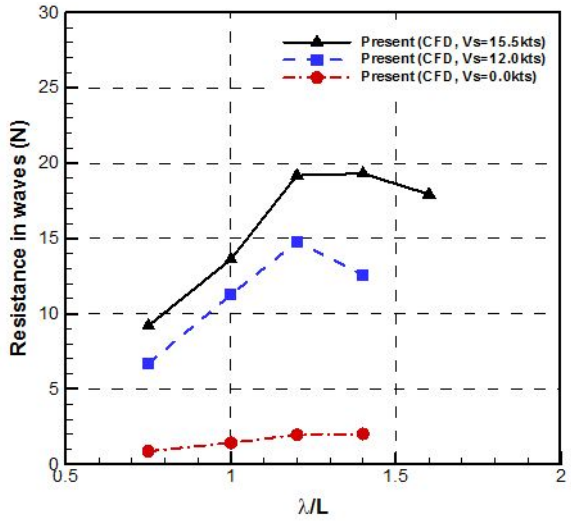

Fig. 11. 0th order term of harmonic resistance force in waves with ship speeds.

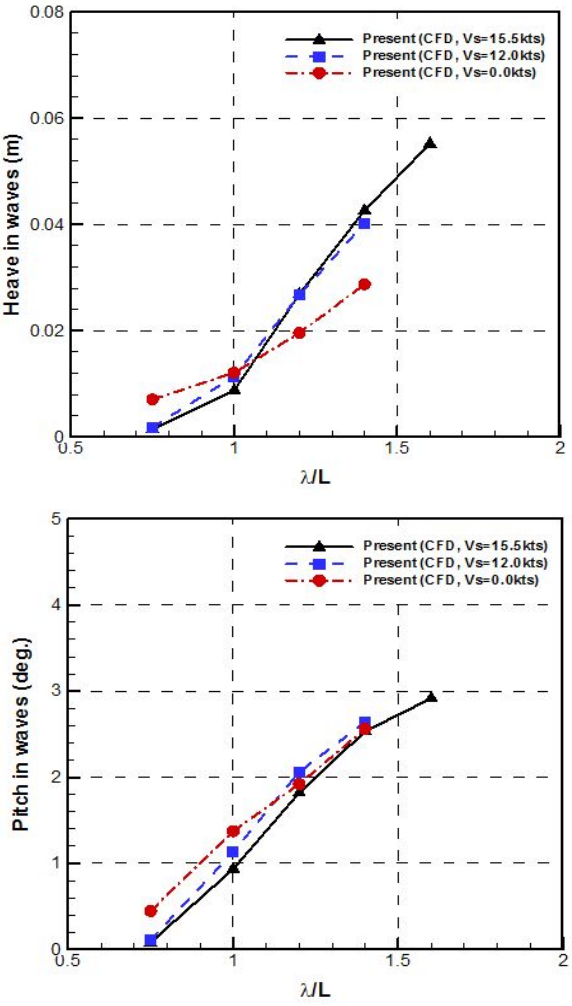

Fig. 12. 1st order terms of harmonic heave and pitch motions with ship speeds.

methods show good agreements. Therefore it is demonstrated that the added resistance and ship motions can be predicted reliably by using current numerical approaches.

Also 0th and 1st order harmonic terms of the resistance force and heave and pitch amplitudes by CFD are compared for ship speeds as shown in Fig. 11 and 12. Total resistance in waves is increasing with increasing ship speed due to the increase of the calm water resistance and the added resistance in waves because of augmented ship motions.

However 1st order harmonic terms of the heave and pitch motion are in similar range of magnitudes and for short wave length (< λ/L=1) heave and pitch motions at Vs=0kts are higher than other ship speeds.

For a resonant case (λ/L=1.2) at Vs=12kts, snapshots of the wave elevation and the vessel movements are presented at t/Te=0.5, when the added resistance is biggest, for operating and zero ship speeds in Fig. 13. Green water and bow slamming are seen at Vs=12kts as shown in Fig. 13(a), while fluctuations of the wave elevation around bow and stern at Vs=0kts are bigger than those at 12kts as presented in Fig. 13(b).

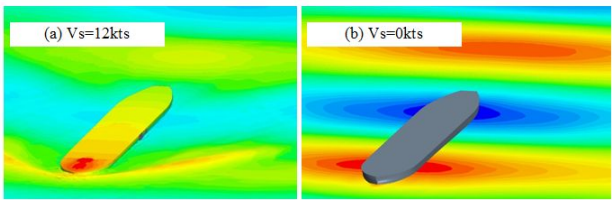

Fig. 13. Free surface elevation over one period of encounter (t/Te=0.5, λ/L=1.2).

Time histories of the resistance force and the ship vertical motions over an encounter period are compared for three ship speeds as shown in Fig. 14. It is found that the oscillation magnitudes of the resistance force at 0kts are bigger than other speeds even though the 0th order term of the resistance force is much lower than other sip speeds in Fig. 11, the 1st order terms of the heave and pitch are similar at λ/L=1.2 in Fig. 11 and 12 and even heave at t/Te=0.5 are almost 0 and pitch amplitudes are negative as stern trim without green water as presented in Fig. 13 and 14. It is deduced that the bigger oscillation of the added resistance at Vs=0kts than other speeds is affected more by the wave height around bow of the ship than the ship vertical motions or green water if the ship has no speed or is on station. Therefore it should be considered that the ship would be carefully operated at ports or in coastal areas especially in heavy wave and wind conditions because the added resistance at zero

speed would be bigger than design and operating speed. Also it should be noted that there are serious concerns regarding the ship manoeuvrability at low speed in restricted areas in adverse weather conditions (Shigunov and Papanikolaou, 2014).

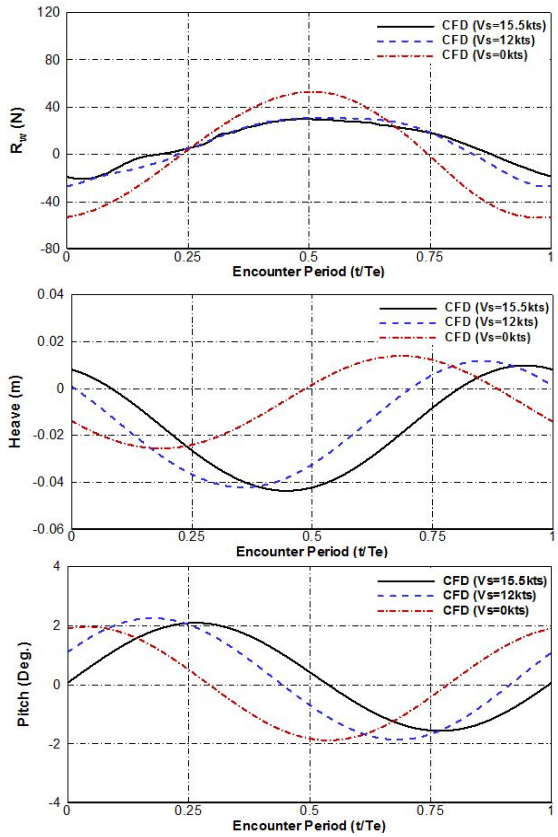

Fig. 14. Resistance, heave and pitch amplitudes over one period of encounter (λ/L=1.2).

5. Conclusions

The added resistance and the ship vertical motions (heave and pitch) in regular head waves have been simulated by the unsteady RANS and the 3-D potential flow methods for a wide range of wave conditions at three ship speeds which are design speed (Vs=15.5kts) as validation study including grid convergence test as well as operating (Vs=12kts) and zero (Vs=0kts) speeds taking into account the ship slow steaming speed and harbour conditions, respectively. Time histories of the resistance and the ship motions in waves calculated by CFD are analysed at each ship speed and the relationship of the resistance force and the ship motions are investigated with unsteady wave patterns and viscous effect.

Firstly appropriate mesh system can be found from grid convergence test for CFD simulations and the resistance and the ship motions in waves in time domain by CFD are oscillating well periodically corresponding to the encounter period for each test case.

Secondly the computation results of the added resistance and the ship motions in regular waves by CFD and 3-D potential methods are in good agreement with experiments at design speed except for pitch motion which is overestimated by 3-D potential method for pick and long waves due to the AFS formulation and is underestimated slightly by CFD for the range of wave length (λ/L) from 1 to 1.4 because of the adoption of the non-inertial reference frame. Wave snapshots and the vessel movements are investigated with time history data of the resistance force and vertical motions over an encounter period. For the case no. C10 (Vs=15.5kts, λ/L=1.2), the biggest resistance in waves appeared when bow slamming is seen apparently at the moment wave height is high around bow and the ship has the biggest sinkage even though pitch amplitude is almost zero after the bow trim.

Thirdly 0th and 1st order harmonic terms of the resistance force and the ship vertical motions calculated by CFD are compared for three ship speeds. The resistance forces are bigger as ship speed is faster, however the heave and pitch motions are in similar range of magnitudes and even higher at Vs=0kts than other ship speeds for relatively short wave length (< λ/L=1).

Finally for a resonant test case (λ/L=1.2) for operating speed, the wave elevation and the ship movements are examined for operating and zero speed. When the ship has the biggest added resistance, bow slamming and green water can be found for operating speed, while the high and low wave elevations around bow and stern respectively are seen clearly for zero speed without the phenomena of water on deck. From the comparison of the time histories of the resistance and the ship motions over an period of encounter, the oscillation magnitudes of the resistance force at Vs=0kts are bigger than other ship speeds although the 0th order term of the resistance force is much lower than other sip speeds, which is likely that the resistance in waves for ship at zero speed is affected by wave elevation around bow and stern more than ship vertical motions because the ship is more likely to be driven by wave conditions. Therefore it should be noted that ships would be carefully operated at ports or in coastal areas especially in heavy wave and wind conditions because the added resistance at zero speed would be bigger than design and operating speed and there are

serious concerns regarding the ship manoeuvrability at low speed in restricted areas in adverse weather conditions.

For the future work, the correlation and analysis in time domain for the added resistance and the ship motions should be investigated further, especially for the ship operating speed as well as the zero speed considering harbour conditions for various wave conditions.

References

[1] Arribas, F. P.(2007), Some methods to obtain the added resistance of a ship advancing waves, Ocean Eng., 34, pp. 946-955.

[2] Bøckmann, A., C. Pâkozdi, T. Kristiansen, H. Jang and J. Kim(2014), An experimental and computational development of a benchmark solution for the validation of numerical wave tank, Proceedings of the ASME 2014, OMAE2014 -24710, pp. 1-14.

[3] Deng, G. B., A. Leroyer, E. Guilmineau, P. Queutey, M. Visonneau and J. Wackers(2010), Verification and validation for unsteady computation. Gothenburg 2010: A workshop on CFD in ship hydrodynamics, pp. 237-259.

[4] Faltinsen, O. M., K. J. Minsaas, N. Liapis and S. O. Skjørdal(1980), Prediction of resistance and propulsion and propulsion of a ship in a seaway, Proceeding of 13th Sym. Naval Hydrodynamics, Tokyo, pp. 505-529.

[5] Gerritsma, J. and W. Beukelman(1972), Analysis of the resistance increase in waves in a fast cargo ship, Intern. Shipbuilding Progr. 19(217), pp. 285-93.

[6] Havelock, T. H.(1937), The resistance of a ship among waves, Proc. Roy. Soc. London A, 161, pp. 299-308.

[7] IMO(2012), International Maritime Organisation, Interim guidelines for the calculation of the coefficient fw for decrease in ship speed in a representative sea condition for trial use, MEPC.1/Circ.796.

[8] ITTC(2014), International Towing Tank Conference, The specialist committee on seakeeping-final report and recommendations to the 27th ITTC, Copenhagen.

[9] Joncquez, S. A. G.(2009), Second-order forces and moments acting on ships in waves, Ph.D. thesis, Technical University of Denmark.

[10] Joosen, W. P. A.(1966), Added resistance of ships in waves. Proc. 6th Symp. Naval Hydrodynamics, Wasington, D.C., pp. 23-34.

[11] Kim, H. T., C. B. Hong, G. H. Lee and B. K. Kim(2015), Prediction of added resistance of a ship in waves using computational fluid dynamics. In: Proceedings of the Annual Spring Conference, SNAK, Korea, pp. 465-478.

[12] Kim, H. T., J. J. Kim, N. Y. Choi and G. H. Lee(2014), A study on the operating trim, shallow water and wave effect. In: Proceedings of the Annual Autumn Conference, SNAK, Korea, pp. 631–637.

[13] Kim, K. H., Y. Kim and Y. Kim(2007), WISH JIP project report and manual, Marine Hydrodynamic Laboratory, Seoul University.

[14] Kim, K. H., M. G. Seo and Y. H. Kim(2012), Numerical analysis on added resistance of ships. International Journal of Offshore and Polar Engineering 22, pp. 21-29.

[15] Kim, M. G. and D. W. Park(2015), A study on the green ship design for ultra large container ship, Journal of the Korean Society of Marine Environment & Safety, Vol. 21, No. 5, pp. 558-570.

[16] Kim, Y. C., K. S. Kim, J. Kim, Y. S. Kim, S. H. Van and Y. H. Jang(2015), Calculation of added resistance in waves for KVLCC2 and its modified hull form using RANS-based method. In: Proceedings of the Twenty-fifth International Ocean and Polar Engineering Conference, Hawaii, USA, pp. 924–930.

[17] Kwon, Y. J.(2008), Speed loss due to added resistance in wind and waves, the Naval Architect 3, pp. 14-16.

[18] Larssson L., F. Stern and M. Visonneau(2010), Experimental data from Osaka University. In: Proceedings of a workshop on numerical ship hydrodynamics, Gothenburg, Sweden, pp. 137-145.

[19] Lee, J. H., M. G. Seo, D. M. Park, K. K. Yang, K. H. Kim and Y. Kim(2013), Study on the effects of hull form on added resistance. In: Proceeding of the 12th International Symposium on Practical Design of Ships and Other Floating Structures (PRADS2013), Changwon, Korea, pp. 329-337.

[20] Lee, S. M.(2015), Experimental study on added resistance of VLCC for ship's operating condition in waves, Journal of the Korean Society of Marine Environment & Safety, Vol. 21, No. 3, pp. 240-245.

[21] Liu, S., A. Papanikolaou and G. Zaraphonitis(2011), Prediction of added resistance of ships in waves, Ocean Engineering 38, pp. 641-650.

[22] MARIN(2009), Maritime Research Institute Netherlands, PRECAL V6.5 Theory Manual, MARIN Report, 17926-2-CPS.

[23] Maruo, H.(1960), The drift of a body floating on waves, Journal of Ship Research, 4(3), pp. 1-10.

[24] Moctar, B., J. Kaufmann, J. Ley, J. Oberhagemann, V. Shigunov and T. Zorn(2010), Prediction of ship resistance and ship motions using RANSE, Gothenburg 2010: A workshop on CFD in ship hydrodynamics.

[25] Newman, J. N.(1967), The drift force and moment on ships in waves. Journal of Ship Research, Vol. 11, pp. 51-60.

[26] Park, D. M., M. G. Seo, J. H. Lee, K. K. Yang and Y. H. Kim(2014), Systematic experimental and numerical analysis on added resistance in waves, Journal of the Society of Naval Architects of Korea, 51(6). pp. 459-479.

[27] Prpić-Oršić, J. and O. M. Faltinsen(2012), Estimation of ship speed loss and associated CO2 emissions in a seaway, Ocean Engineering 44, pp. 1-10.

[28] Sadat-Hosseini H., P. M. Carrica, H. Kim, Y. Toda and F. Stern(2010), URANS simulation and validation of added resistance and motions of the KVLCC2 crude carrier with fixed and free surgte conditions, Gothenburg 2010: A workshop on CFD in ship hydrodynamics.

[29] Sadat-Hosseini H., P. Wu, P. M. Carrica, H. Kim, Y. Toda and F. Stern(2013), CFD verification and validation of added resistance and motions of KVLCC2 with fixed and free surge in short and long head waves, Ocean Eng. 48, pp. 240-273.

[30] Salvesen, N., E. O. Tuck and O. M. Faltinsen(1970), Ship motions and sea loads. SNAME, Jersey City, pp. 1-30.

[31] Shen, Z. and D. Wan(2012), RANS computations of added resistance and motions of ships in head waves, In: Proceedings of 22nd International Offshore and Polar Engineering Conference, Rhodes, Greece, pp. 1096-1103.

[32] Shigunov, V. and A. Papanikolaou(2014), Criteria for minimum powering and maneuverability in adverse weather conditions, The 14th International Ship Stability Workship (ISSW), Kuala Lumbur, Malasia, pp. 174-184.

Received : 2016. 06. 17.
Revised : 2016. 08. 09. (1st)
: 2016. 08. 16. (2nd)
Accepted : 2016. 08. 29.